

## BRIEF COMMUNICATIONS

## Crowd synchrony on the Millennium Bridge

Footbridges start to sway when packed with pedestrians falling into step with their vibrations.

Soon after the crowd streamed on to London's Millennium Bridge on the day it opened, the bridge started to sway from side to side: many pedestrians fell spontaneously into step with the bridge's vibrations, inadvertently amplifying them. Here we model this unexpected and now notorious phenomenon — which was not due to the bridge's innovative design as was first thought — by adapting ideas originally developed to describe the collective synchronization of biological oscillators such as neurons and fireflies. Our approach should help engineers to estimate the damping needed to stabilize other exceptionally crowded footbridges against synchronous lateral excitation by pedestrians.

Existing theories<sup>1–6</sup> of what happened on the bridge's opening day focus on the wobbling of the bridge but have not addressed the crowd-synchronization dynamics. In our approach, wobbling and synchrony are inseparable. They emerge together, as dual aspects of a single instability mechanism, once the crowd reaches a critical size.

We model the bridge as a weakly damped and driven harmonic oscillator

$$M \frac{d^2 X}{dt^2} + B \frac{dX}{dt} + KX = G \sum_{i=1}^N \sin \Theta_i \quad (1)$$

where  $X(t)$  is the displacement of the relevant lateral mode, and  $M$ ,  $B$  and  $K$  are its modal mass, damping and stiffness, respectively (Fig. 1). Each pedestrian  $i = 1, \dots, N$  imparts an alternating sideways force  $G \sin \Theta_i$  to the bridge, where  $G$  is the maximum force and the phase  $\Theta_i(t)$  increases by  $2\pi$  during a full left/right walking cycle.

The bridge's movement, in turn, is assumed to alter each pedestrian's gait according to

$$\frac{d\Theta_i}{dt} = \Omega_i + C A \sin(\Psi - \Theta_i + \alpha) \quad (2)$$

where the frequencies  $\Omega_i$  are randomly distributed with a density  $P(\Omega)$ , reflecting the diversity of natural footfall rates across the population;  $C$  quantifies pedestrians' sensitivity to bridge vibrations of amplitude  $A(t)$  and phase  $\Psi(t)$  (defined such that  $X = A \sin \Psi$ ,  $dX/dt = \Omega_0 A \cos \Psi$ , where  $\Omega_0 = \sqrt{K/M}$  is the

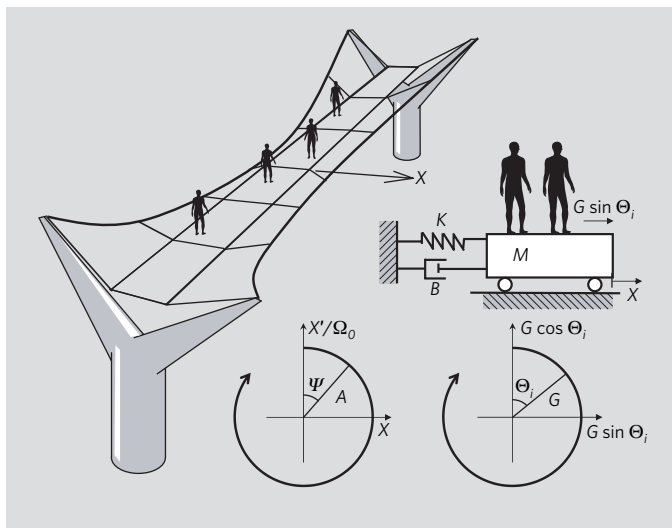


**Figure 1 | Effect of pedestrian crowding on London's Millennium Bridge.** The resonant lateral mode of vibration of the bridge (left) can be represented by a mass-spring-damper system (top, right). The angular phases (bottom) for the bridge displacement  $X$  (left) and the individual pedestrian forces,  $G \sin \Theta_i$  (right), are indicated (see text for definitions of variables).

bridge's resonant frequency); and  $\alpha$  is a phase lag parameter. Equation (2) is hypothetical but testable (see supplementary information), and is consistent with the known response of other biological rhythms to weak periodic stimuli<sup>7,8</sup>.

To illustrate the dynamics inherent in the model, Fig. 2 shows a simulation of a controlled experiment<sup>2</sup> performed on the Millennium Bridge. As more and more people walk on to the deck (Fig. 2a), there is no hint of

### Figure 2 | Simulated outbreak of wobbling and crowd synchronization on the Millennium Bridge.

**a**, Number of pedestrians,  $N$ , slowly increasing stepwise, as used in a diagnostic wobble test<sup>2</sup> on the bridge's north span in December 2000. **b**, Predicted amplitude  $A = (X^2 + (\Omega_0^{-1} dX/dt)^2)^{1/2}$  of the bridge's resulting lateral vibrations. **c**, Predicted degree of phase coherence among the pedestrians, as measured by the order parameter<sup>9,10</sup>  $R = N^{-1} |\sum_{i=1}^N \exp(i\Theta_i)|$ . For small crowds, walkers are desynchronized and randomly phased: hence  $R$  fluctuates and decays as  $R \approx N^{-1/2}$ . At a critical crowd size (dashed lines in **a–c**), the bridge starts to sway and the crowd starts to synchronize, with each process pumping the other in a positive feedback loop;  $R$  and  $A$  follow parallel time-courses (**b, c**), maintaining an almost constant ratio. This predicts the empirical observation<sup>1</sup> that the crowd drives the bridge with a force proportional to the bridge's velocity (see supplementary information for details).

instability until the crowd reaches a critical size,  $N_c$ , after which wobbling and synchrony erupt simultaneously (Fig. 2b, c).

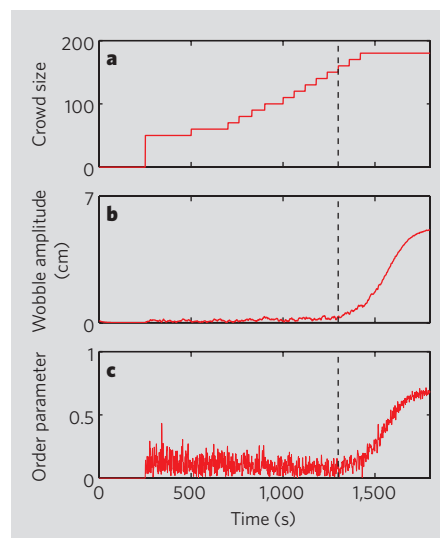
We can calculate  $N_c$  analytically, using methods<sup>8–10</sup> created to study large systems of biological oscillators (see supplementary information). To take the simplest case, suppose  $\alpha = \pi/2$  and  $P(\Omega)$  is symmetrical about  $\Omega_0$  (also a 'worst case' for the bridge, in the sense that pedestrians then drive it most efficiently). We find

$$N_c = \frac{4\varsigma}{\pi} \left( \frac{K}{GC P(\Omega_0)} \right) \quad (3)$$

where  $\varsigma = B/\sqrt{4MK}$  is the damping ratio. All the parameters have known values, except for  $C$ . Comparing our simulations with data obtained from crowd tests on the Millennium Bridge<sup>2</sup>, we estimate  $C \approx 16 \text{ m}^{-1} \text{ s}^{-1}$ . Then, with no further

adjustable parameters, the model predicts the synchronization timescale and the characteristic amplitude of the wobbles shown in Fig. 2 and in the actual experiments<sup>1,2</sup>. It also accounts for the previously unexplained empirical observation<sup>1</sup> that the excitation force generated by the crowd grows linearly with the bridge's amplitude (for calculations, see supplementary information).

By generalizing ideas that were developed in



mathematical biology, we have provided a unified picture of what happened on the Millennium Bridge five years ago, both for the bridge vibrations and the crowd dynamics. The approach suggested here may also prove useful for estimating the damping needed to safeguard other bridges, present and future, against synchronous lateral excitation by pedestrians.

**Steven H. Strogatz\***, **Daniel M. Abrams\***,  
**Allan McRobie†**, **Bruno Eckhardt‡**, **Edward Ott‡**

\*Department of Theoretical and Applied Mechanics, Cornell University, Ithaca, New York 14853-1503, USA

e-mail: strogatz@cornell.edu

†Department of Engineering, University of Cambridge, Cambridge CB2 1PZ, UK

‡University of Maryland, College Park, Maryland 20742, USA

SFachbereich Physik, Philipps-Universität Marburg, 35032 Marburg, Germany

1. Dallard, P. *et al. Struct. Eng.* **79**, 17–33 (2001).
2. Dallard, P. *et al. J. Bridge Eng.* **6**, 412–417 (2001).
3. McRobie, A., Morgenthal, G., Lasenby, J. & Ringer, M. *Proc. Inst. Civ. Eng. Bridge Eng.* **156**, 71–79 (2003).
4. Roberts, T. M. *Proc. Inst. Civ. Eng. Bridge Eng.* **156**, 155–160 (2003).
5. Newland, D. E. *Proc. Inst. Mech. Eng.* **218**, 477–492 (2004).
6. Nakamura, S. *J. Struct. Eng.* **130**, 32–37 (2004).
7. Glass, L. & Mackey, M. C. *From Clocks to Chaos: The Rhythms of Life* (Princeton Univ. Press, Princeton, 1988).
8. Winfree, A. T. *The Geometry of Biological Time* 2nd edn (Springer, New York, 2001).
9. Kuramoto, Y. *Chemical Oscillations, Waves and Turbulence* (Springer, Berlin, 1984).
10. Strogatz, S. H. *Physica D* **143**, 1–20 (2000).

**Supplementary information** accompanies this communication on Nature's website.

**Competing financial interests:** declared none.  
doi:10.1038/43843a

associated liquids (water and alcohols) with time can be attributed to flow-induced solvent ordering or the formation of bubbles (our unpublished results).

We conclude that these high fluid velocities are possible because of a frictionless surface at the carbon-nanotube wall. This result could be explained in conventional terms of slip lengths, which are remarkably long. The slip length is an extrapolation of the extra pore radius required to give zero velocity at a hypothetical pore wall (the boundary condition for conventional materials). The observed slip lengths (3–70  $\mu\text{m}$ ) are much longer than the pore radius (3.5 nm) that is consistent with a nearly frictionless interface. The slip length decreases as solvents become more hydrophobic (Table 1), which indicates stronger interaction with the carbon-nanotube wall. The observed flow velocities for water (10–44  $\text{cm s}^{-1}$ ) are close to the extrapolated rate predicted for water flow through single-walled carbon nanotubes (about 90  $\text{cm s}^{-1}$ )<sup>4</sup>. Butane flows through carbon nanotubes at about 26  $\text{cm s}^{-1}$  (ref. 6), which is consistent with our measurement for hexane.

These results show that the speed of fluid flow through the aligned carbon-nanotube membrane approaches that through biological channels. The membrane fabrication is scalable to large areas, which could be useful industrially for chemical separations; chemical functionality is near the core entrance<sup>9</sup> and each side of the membrane can be independently modified with different functional groups<sup>10</sup>. These advantages also make the aligned carbon-nanotube membrane a promising mimic of protein channels for transdermal drug delivery and selective chemical sensing.

**Mainak Majumder\***, **Nitin Chopra\***,  
**Rodney Andrews†**, **Bruce J. Hinds\***

\*Chemical and Materials Engineering Department, University of Kentucky, Lexington, Kentucky 40506, USA

e-mail: bjhinds@engr.uky.edu

†Center for Applied Energy Research, Lexington, Kentucky 40511, USA

1. Hille, B. *Ionic Channels of Excitable Membranes* (Sinauer, Sunderland, Massachusetts, 1984).
2. Jirage, K. B., Hulstee, J. C. & Martin, C. R. *Science* **278**, 655–658 (1997).
3. Klein, E. J. *Membr. Sci.* **179**, 1–27 (2000).
4. Hummer, G., Rasaiah, J. C. & Noworyta, J. P. *Nature* **414**, 188–190 (2001).
5. Sokhan, V. P., Nicholson, D. & Quirke, N. *J. Chem. Phys.* **117**, 8531–8539 (2002).
6. Skoulidis, A. I., Ackerman, D. M., Johnson, J. K. & Sholl, D. S. *Phys. Rev. Lett.* **89**, 185901 (2002).
7. Mao, Z. & Sinnott, S. B. *J. Phys. Chem. B* **105**, 6916–6924 (2001).
8. Hinds, B. J. *et al. Science* **303**, 62–65 (2004).
9. Majumder, M., Chopra, N. & Hinds, B. J. *J. Am. Chem. Soc.* **127**, 9062–9067 (2005).
10. Chopra, N., Majumder, M. & Hinds, B. J. *Adv. Funct. Mater.* **15**, 858–864 (2005).

**Supplementary information** accompanies this communication on Nature's website.

**Competing financial interests:** declared online.  
doi:10.1038/43844a

## NANOSCALE HYDRODYNAMICS

# Enhanced flow in carbon nanotubes

Nanoscale structures that could mimic the selective transport and extraordinarily fast flow possible in biological cellular channels would have a wide range of potential applications. Here we show that liquid flow through a membrane composed of an array of aligned carbon nanotubes is four to five orders of magnitude faster than would be predicted from conventional fluid-flow theory. This high fluid velocity results from an almost frictionless interface at the carbon-nanotube wall.

Biological channels act as chemically selective gatekeepers and have protein walls that allow extremely rapid transit<sup>1</sup>. Nanometre-scale pores with chemical selectivity have been prepared<sup>2,3</sup> but fluid flow through them is slow: this limitation is predicted by the Hagen–Poiseuille equation and is because conventional laminar flow has zero fluid velocity at the pore walls.

In theory, the flow of molecules inside carbon nanotubes could be much faster. Water should be able to flow fast through hydrophobic single-walled carbon nanotubes because the process creates ordered hydrogen bonds between the water molecules<sup>4</sup>. Ordered hydrogen bonds between water molecules and the weak attraction between the water and smooth carbon-

nanotube graphite sheets should then result in almost frictionless and very rapid flow<sup>4</sup>. If a theoretical volume rate comparable to that of the protein channel aquaporin-1 (ref. 4) is divided by the carbon-nanotube cross-sectional area, the expected water flow velocity is about 90  $\text{cm s}^{-1}$ . Fast flow velocities are also predicted just from the frictionless nature of the carbon-nanotube walls<sup>5</sup> and from the rapid diffusion of hydrocarbons<sup>6,7</sup>.

To realize these high flow velocities, we used a freshly fabricated membrane consisting of aligned multiwalled carbon nanotubes, with graphitic inner cores (diameter about 7 nm) and a high area density ( $5 \times 10^{10}$  per  $\text{cm}^2$ ), crossing a solid polystyrene film<sup>8</sup>. We measured the flow of water and a variety of solvents through this membrane at about 1 atm applied pressure (Table 1). In a control experiment, we verified that no macroscopic defects were present in the membrane and determined the available pore area (see supplementary information).

We found that the flow rates are four to five orders of magnitude faster than conventional fluid flow would predict through pores of 7 nm diameter. Contrary to predictions based on hydrodynamics, the flow rate does not decrease with increased viscosity (compare hexane and water in Table 1). The results also indicate that flow velocity, when adjusted for differences in viscosity, increases for more hydrophilic fluids. The flow of hydrogen-bonded fluids decreases after a few minutes, but this does not occur with alkanes or aqueous solutions of potassium chloride. Reduction in the flow of

**Table 1 | Pressure-driven flow through aligned MWCNT membrane**

Liquid	Initial permeability*	Observed flow velocity†	Expected flow velocity†	Slip length (nm)
Water	0.58	25	0.00057	54
	1.01	43.9	0.00057	68
	0.72	9.5	0.00015	39
Ethanol	0.35	4.5	0.00014	28
iso-Propanol	0.088	1.12	0.00077	13
Hexane	0.44	5.6	0.00052	9.5
Decane	0.053	0.67	0.00017	3.4

MWCNT, multiwalled carbon nanotube. For details of methods, see supplementary information. \*Units,  $\text{cm}^3$  per  $\text{cm}^2$  min bar. †Flow velocities in  $\text{cm s}^{-1}$  at 1 bar. Expected flow velocity is that predicted from conventional flow.